

Fuzzy Chamfer Distance and its Probabilistic Formulation for Visual Tracking

Yonggang Jin*[†] Farzin Mokhtarian[†] Mirosław Bober* John Illingworth[†]
*Visual Information Laboratory [†]Centre for Vision, Speech and Signal Processing
Mitsubishi Electric ITE B.V., UK University of Surrey, UK
{yonggang.jin, miroslaw.bober}@vil.ite.mee.com {f.mokhtarian, j.illingworth}@surrey.ac.uk

Abstract

The paper presents a fuzzy chamfer distance and its probabilistic formulation for edge-based visual tracking. First, connections of the chamfer distance and the Hausdorff distance with fuzzy objective functions for clustering are shown using a reformulation theorem. A fuzzy chamfer distance (FCD) based on fuzzy objective functions and a probabilistic formulation of the fuzzy chamfer distance (PFCD) based on data association methods are then presented for tracking, which can all be regarded as reformulated fuzzy objective functions and minimized with iterative algorithms. Results on challenging sequences demonstrate the performance of the proposed tracking method.

1. Introduction

This paper focuses on edge-based visual tracking. Previous work on edge-based tracking includes contour tracking with Kalman filters [5], particle filters [17], EM algorithms [22], and edge template based tracking with the chamfer distance (CD) [24] or the Hausdorff distance (HD) [15]. The CD and the HD were initially used for feature-based object recognition [14, 16, 23, 11], where the CD was employed for object detection in [11] and the HD was used with efficient algorithms based on the distance transform (DT) [7] to locate objects under translation [14], translation-scaling [16] and affine transform [23]. A probabilistic formulation of the HD was presented in [20] where a likelihood was proposed for ML matching. A modified HD was presented in [10]. Edge template based tracking with a partial forward HD was proposed in [15]. Hand tracking with a multi-channel CD for edge feature, in combination with skin color feature, was presented in [24]. It can be noted that usage of the CD/HD in previous work relies on the DT so that multi-resolution search or particle filters can be applied. However, for the DT only low dimensional feature vectors can be used as the complexity of the DT grows rapidly with the dimensionality of feature vectors. In ad-

dition, the complexity of multi-resolution search or particle filters also grows rapidly with the dimensionality of state vectors.

This paper presents a fuzzy chamfer distance and its probabilistic formulation for edge-based visual tracking. First, connections of the CD/HD with fuzzy objective functions for clustering [4] are shown using a reformulation theorem [13]. A fuzzy chamfer distance (FCD) based on fuzzy objective functions is then introduced, which can be regarded as a reformulated fuzzy objective function and minimized with an iterative algorithm. A probabilistic formulation of the fuzzy chamfer distance (PFCD) based on data association methods is further presented, which can also be regarded as a reformulated fuzzy objective function and minimized with an iterative algorithm. It extends the work in [18], which can be regarded as tracking with a reverse PFCD, to tracking with a forward PFCD in the same spirit of the previous work in [15, 20] but in a tractable approach using iterative algorithms. In addition, the forward and reverse FCD/PFCD can be combined for more robust tracking using iterative algorithms. Note that for the FCD/PFCD, the DT is not useful as distances from all model samples to all measurements have to be computed. Higher dimensional feature vectors can be employed, as distances of feature vectors only need to be computed once and are then used in iterative algorithms. Due to a monotonicity property of the iterative algorithm, it can seek the mode of likelihoods or posteriors despite high dimensional state space and sharply peaked likelihoods, which may be difficult for tracking with multi-resolution search and particle filters.

The organization of the paper is as follows. Fuzzy objective functions are introduced in Section 2; Tracking with the FCD/PFCD is presented in Section 3; Results are given in Section 4 and the paper is concluded in Section 5.

2. Fuzzy objective functions

2.1. Chamfer distance and Hausdorff distance

Chamfer distance Given a set of M points $\mathbf{M} = \{\mathbf{m}_j\}_{j=1}^M$ and a set of N points $\mathbf{Z} = \{\mathbf{z}_i\}_{i=1}^N$, the directed CD from

\mathbf{M} to \mathbf{Z} is

$$D_{CD}(\mathbf{M}, \mathbf{Z}) = \frac{1}{M} \sum_{j=1}^M d(\mathbf{m}_j, \mathbf{Z}) \quad (1)$$

where $d(\mathbf{m}_j, \mathbf{Z}) = \min_i \|\mathbf{m}_j - \mathbf{z}_i\|$. If \mathbf{M} is regarded as a model and \mathbf{Z} as measurements, $D_{CD}(\mathbf{M}, \mathbf{Z})$ is the forward CD from \mathbf{M} to \mathbf{Z} whereas the reverse CD from \mathbf{Z} to \mathbf{M} is $D_{CD}(\mathbf{Z}, \mathbf{M})$ after swapping \mathbf{M} and \mathbf{Z} .

The thresholded directed CD, which is more robust to outliers, is given by

$$D_{CD}^\delta(\mathbf{M}, \mathbf{Z}) = \frac{1}{M} \sum_{j=1}^M \min(\delta, d(\mathbf{m}_j, \mathbf{Z})) \quad (2)$$

where δ is a distance threshold. Likewise, if \mathbf{M} is regarded as a model and \mathbf{Z} as measurements, $D_{CD}^\delta(\mathbf{M}, \mathbf{Z})$ is the thresholded forward CD from \mathbf{M} to \mathbf{Z} whereas the thresholded reverse CD from \mathbf{Z} to \mathbf{M} is $D_{CD}^{\delta'}(\mathbf{Z}, \mathbf{M})$ with reverse threshold δ' .

Hausdorff distance The directed HD is [14]

$$D_{HD}(\mathbf{M}, \mathbf{Z}) = \max_j d(\mathbf{m}_j, \mathbf{Z}) \quad (3)$$

If \mathbf{M} is regarded as a model and \mathbf{Z} as measurements, $D_{HD}(\mathbf{M}, \mathbf{Z})$ is the forward HD from \mathbf{M} to \mathbf{Z} whereas the reverse HD from \mathbf{Z} to \mathbf{M} is $D_{HD}(\mathbf{Z}, \mathbf{M})$. The symmetric HD is $\mathcal{D}_{HD}(\mathbf{M}, \mathbf{Z}) = \max(D_{HD}(\mathbf{M}, \mathbf{Z}), D_{HD}(\mathbf{Z}, \mathbf{M}))$.

To be more robust to outliers, a partial HD is often used instead and the directed partial HD is

$$D_{HD}^q(\mathbf{M}, \mathbf{Z}) = q^{th} d(\mathbf{m}_j, \mathbf{Z}) \quad (4)$$

where $q \in [0, 1]$ and $q^{th} d(\mathbf{m}_j, \mathbf{Z})$ denotes the q^{th} quantile value of $\{d(\mathbf{m}_j, \mathbf{Z})\}_{j=1}^M$ in ascending order and it becomes the maximum if $q = 1$ and the median if $q = \frac{1}{2}$. Likewise, if \mathbf{M} is regarded as a model and \mathbf{Z} as measurements, $D_{HD}^q(\mathbf{M}, \mathbf{Z})$ is the forward partial HD with quantile q and $D_{HD}^{q'}(\mathbf{M}, \mathbf{Z})$ is the reverse partial HD with quantile q' . The partial HD is $\mathcal{D}_{HD}^{q,q'}(\mathbf{M}, \mathbf{Z}) = \max(D_{HD}^q(\mathbf{M}, \mathbf{Z}), D_{HD}^{q'}(\mathbf{Z}, \mathbf{M}))$.

2.2. Fuzzy objective functions for clustering

Fuzzy c-means (FCM) clustering FCM was presented in [4] with an objective function

$$J_{FCM}(\mathbf{Z}, \mathbf{M}; \mathbf{Q}) = \sum_{i=1}^N \sum_{j=1}^M q_{i,j}^r d(\mathbf{z}_i, \mathbf{m}_j) \quad (5)$$

subject to $\sum_{j=1}^M q_{i,j} = 1$

where $\mathbf{Z} = \{\mathbf{z}_i\}_{i=1}^N$ are N samples, $\mathbf{M} = \{\mathbf{m}_j\}_{j=1}^M$ are M prototypes, $d(\mathbf{z}_i, \mathbf{m}_j)$ is the distance from sample \mathbf{z}_i to prototype \mathbf{m}_j , $\mathbf{Q} = \{q_{i,j}\}_{i=1}^N$, $q_{i,j}$ is the membership of sample \mathbf{z}_i in the j th cluster and $r \in [1, \infty)$ is a weighting exponent called the fuzzifier.

To minimize $J_{FCM}(\mathbf{Z}, \mathbf{M}; \mathbf{Q})$, it can be shown that

$$q_{i,j} = \frac{d(\mathbf{z}_i, \mathbf{m}_j)^{\frac{1}{1-r}}}{\sum_{k=1}^M d(\mathbf{z}_i, \mathbf{m}_k)^{\frac{1}{1-r}}} \quad \mathbf{m}_j = \frac{\sum_{i=1}^N q_{i,j}^r \mathbf{z}_i}{\sum_{i=1}^N q_{i,j}^r} \quad (6)$$

Noise clustering (NC) NC was proposed in [9] to make clustering more robust to noise. In NC, noise is considered as a separate class and is represented by a prototype that has a constant distance δ to all samples. The objective function of NC is

$$J_{NC}(\mathbf{Z}, \mathbf{M}; \mathbf{Q}) = \sum_{i=1}^N \left[q_{i,c}^r \delta + \sum_{j=1}^M q_{i,j}^r d(\mathbf{z}_i, \mathbf{m}_j) \right] \quad (7)$$

$$\text{subject to } q_{i,c} + \sum_{j=1}^M q_{i,j} = 1$$

where $q_{i,c}$ is the membership of sample \mathbf{z}_i in the noise cluster. To minimize $J_{NC}(\mathbf{Z}, \mathbf{M}; \mathbf{Q})$, it can be shown that

$$q_{i,j} = \frac{d(\mathbf{z}_i, \mathbf{m}_j)^{\frac{1}{1-r}}}{\sum_{k=1}^M d(\mathbf{z}_i, \mathbf{m}_k)^{\frac{1}{1-r}} + \delta^{\frac{1}{1-r}}} \quad q_{i,c} = \frac{\delta^{\frac{1}{1-r}}}{\sum_{k=1}^M d(\mathbf{z}_i, \mathbf{m}_k)^{\frac{1}{1-r}} + \delta^{\frac{1}{1-r}}} \quad (8)$$

$$\mathbf{m}_j = \frac{\sum_{i=1}^N q_{i,j}^r \mathbf{z}_i}{\sum_{i=1}^N q_{i,j}^r} \quad (9)$$

and if $\delta \rightarrow +\infty$, NC reduces to FCM.

2.3. Reformulated fuzzy objective functions

The reformulation theorem was introduced in [13] by Hathaway and Bezdek to convert an original objective function J to an unconstrained objective function R . According to the reformulation theorem,

- $(\hat{\mathbf{Q}}, \hat{\mathbf{M}})$ globally minimizes $J \Rightarrow \hat{\mathbf{M}}$ globally minimizes R
- $\hat{\mathbf{M}}$ globally minimizes $R \Rightarrow (\hat{\mathbf{Q}}, \hat{\mathbf{M}})$ globally minimizes J
- $(\hat{\mathbf{Q}}, \hat{\mathbf{M}})$ locally minimizes $J \Rightarrow \hat{\mathbf{M}}$ locally minimizes R
- $\hat{\mathbf{M}}$ locally minimizes $R \Rightarrow (\hat{\mathbf{Q}}, \hat{\mathbf{M}})$ locally minimizes J

With the reformulation theorem, it can be shown that the reverse CD, reverse thresholded CD and partial reverse HD are all special cases of reformulated fuzzy objective functions of FCM, NC and fuzzy c-least q th quantile of

squares (FCLQS) clustering respectively.

Fuzzy c-means clustering and chamfer distance

Substitute $q_{i,j}$ in equation (6) into equation (5), the reformulated objective function of FCM is

$$R_{FCM}(\mathbf{Z}, \mathbf{M}) = \sum_{i=1}^N \left[\sum_{j=1}^M d(\mathbf{z}_i, \mathbf{m}_j)^{\frac{1}{1-r}} \right]^{1-r} \quad (10)$$

$$= \sum_{i=1}^N H_{FCM}^r(\mathbf{z}_i, \mathbf{M})$$

where $H_{FCM}^r(\mathbf{z}_i, \mathbf{M}) = \left[\sum_{j=1}^M d(\mathbf{z}_i, \mathbf{m}_j)^{\frac{1}{1-r}} \right]^{1-r}$

is proportional to the *generalized mean* (GM) of distances from sample \mathbf{z}_i to prototypes \mathbf{M} ,

$$F^{-1} \left(\sum_{j=1}^M h_j F(d(\mathbf{z}_i, \mathbf{m}_j)) \right), \sum_{j=1}^M h_j = 1 \quad \text{where}$$

$F(x) = x^{\frac{1}{1-r}}$ is a polynomial and $h_j = \frac{1}{M}$.

Note that if $r \rightarrow 1^+$, then $H_{FCM}^1(\mathbf{z}_i, \mathbf{M}) = \min_j d(\mathbf{z}_i, \mathbf{m}_j)$ is the minimum distance from \mathbf{z}_i to \mathbf{M} . So if \mathbf{M} is regarded as a model whereas \mathbf{Z} as measurements, $R_{FCM}(\mathbf{Z}, \mathbf{M})$ is equivalent to the reverse CD $D_{CD}(\mathbf{Z}, \mathbf{M})$.

Noise clustering and thresholded chamfer distance

Substitute equation (8) into equation (7), the reformulated objective function of NC is

$$R_{NC}(\mathbf{Z}, \mathbf{M}) = \sum_{i=1}^N \left[\delta^{\frac{1}{1-r}} + \sum_{j=1}^M d(\mathbf{z}_i, \mathbf{m}_j)^{\frac{1}{1-r}} \right]^{1-r}$$

$$= \sum_{i=1}^N H_{NC}^r(\mathbf{z}_i, \mathbf{M}) \quad (11)$$

where $H_{NC}^r(\mathbf{z}_i, \mathbf{M}) = \left[\delta^{\frac{1}{1-r}} + \sum_{j=1}^M d(\mathbf{z}_i, \mathbf{m}_j)^{\frac{1}{1-r}} \right]^{1-r}$ is

also proportional to the GM of distances from sample \mathbf{z}_i to all prototypes, \mathbf{M} and the prototype of the noise cluster.

Note that if $r \rightarrow 1^+$, then $H_{NC}^1(\mathbf{z}_i, \mathbf{M}) = \min_j \left(\delta, \min_j d(\mathbf{z}_i, \mathbf{m}_j) \right)$ is the thresholded minimum distance from \mathbf{z}_i to \mathbf{M} . So if \mathbf{M} is regarded as a model whereas \mathbf{Z} as measurements, $R_{NC}(\mathbf{Z}, \mathbf{M})$ is equivalent to the thresholded reverse CD $D_{CD}^\delta(\mathbf{Z}, \mathbf{M})$.

Fuzzy c-least q th quantile of squares (FCLQS) clustering and Hausdorff distance

Fuzzy c-least median of squares (FCLMS) clustering was proposed in [19] and the reformulated objective function of FCLMS is

$$R_{FCLMS}(\mathbf{Z}, \mathbf{M}) = \text{median}_i (H_{FCM}^r(\mathbf{z}_i, \mathbf{M}))$$

Median can be replaced by the q th quantile and it becomes fuzzy c-least q th quantile of squares clustering,

$$R_{FCLQS}^q(\mathbf{Z}, \mathbf{M}) = q_i^{\text{th}} (H_{FCM}^r(\mathbf{z}_i, \mathbf{M}))$$

where if $q = \frac{1}{2}$ FCLQS reduces to FCLMS. If $r \rightarrow 1^+$, $H_{FCM}^1(\mathbf{z}_i, \mathbf{M}) = \min_j d(\mathbf{z}_i, \mathbf{m}_j)$ and regard \mathbf{M} as a

model whereas \mathbf{Z} as measurements, then $R_{FCLQS}^q(\mathbf{Z}, \mathbf{M})$ is equivalent to the partial reverse HD $D_{HD}^q(\mathbf{M}, \mathbf{Z})$. However, there are no corresponding original objective functions of FCLMS and FCLQS that can be minimized analytically as those of FCM and NC. Some heuristical iterative optimization algorithms or the genetic algorithm [19, 12] are used for minimization.

3. Fuzzy chamfer distance and its probabilistic formulation for visual tracking

Before introducing the fuzzy chamfer distance and its probabilistic formulation for visual tracking, state vector, measurements and models for tracking are described. State vector is denoted as $\mathbf{x}(t) = [x(t) \ y(t) \ a(t) \ b(t)]^T$ where $[x(t) \ y(t)]^T$ is the spatial position of an object center, $a(t)$ and $b(t)$ are the width and height of the object respectively. A second order auto-regressive model is employed as the dynamical model, $\mathbf{x}(t) = \mathbf{A}_1 \mathbf{x}(t-1) + \mathbf{A}_2 \mathbf{x}(t-2) + \mathbf{B}_0 \mathbf{w}(t)$, where $\mathbf{w}(t)$ is Gaussian noise $\mathcal{N}(\mathbf{w}(t); \mathbf{0}, \mathbf{I})$.

3.1. Measurements and Models

Edge measurements are first detected by the Canny edge detector [8]. The gating procedure of Probabilistic Data Association (PDA) is then applied. A validation region is computed based on the predicted state vector using the dynamical model, so only measurements from within the validation region of the predicted state vector are used [2], which are denoted as $\mathbf{Z} = \{\mathbf{z}_i\}_{i=1}^N$ where N is the number of measurements, $\mathbf{z}_i = \begin{bmatrix} \mathbf{u}_i \\ \mathbf{v}_i \end{bmatrix}$, $\mathbf{u}_i = [x_i, y_i]^T$ and $\mathbf{v}_i = \theta_i \in [0, 2\pi)$ are the spatial position and the orientation of the i th edge measurement respectively.

The edge-based object model \mathbf{M} includes a contour model $\mathbf{M}_{con} = \{\mathbf{m}_{con,j}\}_{j=1}^{M_{con}} = \left\{ \begin{bmatrix} \mathbf{u}_{con,j} \\ \mathbf{v}_{con,j} \end{bmatrix} \right\}_{j=1}^{M_{con}}$, which consists of M_{con} contour sample points, and a edge model $\mathbf{M}_{edge} = \{\mathbf{m}_{edge,j}\}_{j=1}^{M_{edge}} = \left\{ \begin{bmatrix} \mathbf{u}_{edge,j} \\ \mathbf{v}_{edge,j} \end{bmatrix} \right\}_{j=1}^{M_{edge}}$, which consists of M_{edge} edge pixels inside the object contour. An ellipse can be used for head tracking and more complex contours can be represented by B-splines [6, 3]. Let $\mathbf{M} = \{\mathbf{m}_j\}_{j=1}^M = \left\{ \{\mathbf{m}_{con,j}\}_{j=1}^{M_{con}}, \{\mathbf{m}_{edge,j}\}_{j=1}^{M_{edge}} \right\}$, $M = M_{con} + M_{edge}$ and later on for brevity, it will not be

specified whether \mathbf{m}_j is from the contour model or the edge model.

3.2. Tracking with the fuzzy chamfer distance

Given N measurements $\mathbf{Z} = \{\mathbf{z}_i\}_{i=1}^N$ and M model samples $\mathbf{M} = \{\mathbf{m}_j\}_{j=1}^M$, the forward FCD from \mathbf{M} to \mathbf{Z} is defined based on the weighted sum of generalized means with a polynomial function $F(x)$,

$$D_{FCD}^F(\mathbf{M}, \mathbf{Z}) = \sum_{j=1}^M \beta_j \left[\left(\omega_c (\delta)^{\frac{1}{1-r}} + \sum_{i=1}^N \omega_i d(\mathbf{m}_j, \mathbf{z}_i)^{\frac{1}{1-r}} \right) \right]^{1-r} \quad (12)$$

where $\omega_c + \sum_{i=1}^N \omega_i = 1$, $d(\mathbf{m}_j, \mathbf{z}_i) = \|\mathbf{m}_j - \mathbf{z}_i\|_{\Sigma}^2 = (\mathbf{u}_j - \mathbf{u}_i)^T \Sigma_{\mathbf{u}}^{-1} (\mathbf{u}_j - \mathbf{u}_i) + (\mathbf{v}_j - \mathbf{v}_i)^T \Sigma_{\mathbf{v}}^{-1} (\mathbf{v}_j - \mathbf{v}_i)$ assuming covariance $\Sigma = \begin{bmatrix} \Sigma_{\mathbf{u}} & \mathbf{0} \\ \mathbf{0} & \Sigma_{\mathbf{v}} \end{bmatrix}$, β_j is the weight of the j th model sample and $\sum_{j=1}^M \beta_j = 1$. Note that if let $r \rightarrow 1^+$, $\beta_j = \frac{1}{M}$ and $\omega_c = \omega_i = \frac{1}{N}$, then $D_{FCD}^F(\mathbf{M}, \mathbf{Z}) = \frac{1}{M} \sum_{j=1}^M \min \left(\delta, \min_i d(\mathbf{m}_j, \mathbf{z}_i) \right)$ reduces to the thresholded forward CD $D_{CD}^{\delta}(\mathbf{M}, \mathbf{Z})$.

By swapping the model and measurements, the reverse FCD is defined as

$$D_{FCD}^R(\mathbf{Z}, \mathbf{M}) = \sum_{i=1}^N \alpha_i \left[\left(\pi_c (\delta')^{\frac{1}{1-r}} + \sum_{j=1}^M \pi_j d(\mathbf{z}_i, \mathbf{m}_j)^{\frac{1}{1-r}} \right) \right]^{1-r} \quad (13)$$

where if $r \rightarrow 1^+$, $\alpha_i = \frac{1}{N}$ and $\pi_c = \pi_j = \frac{1}{M}$, then $D_{FCD}^R(\mathbf{Z}, \mathbf{M}) = \frac{1}{N} \sum_{i=1}^N \min \left(\delta', \min_j d(\mathbf{z}_i, \mathbf{m}_j) \right)$ reduces to the thresholded reverse CD $D_{CD}^{\delta'}(\mathbf{Z}, \mathbf{M})$.

To track with the FCD, model \mathbf{M} is dependent on state vector $\mathbf{x}(t)$ with the aim to minimize the FCD, so $\mathbf{M}(\mathbf{x}(t)) = \{T(\mathbf{m}_j, \mathbf{x}(t))\}_{j=1}^M$, where the transformed j th model sample $T(\mathbf{m}_j, \mathbf{x}(t)) = \begin{bmatrix} T_{\mathbf{u}}(\mathbf{u}_j, \mathbf{x}(t)) \\ \mathbf{v}_j \end{bmatrix}$, $T_{\mathbf{u}}(\mathbf{u}_j, \mathbf{x}(t))$ is the spatial transformation of the spatial position of the j th model sample whereas feature vector \mathbf{v}_j is assumed to be unchanged.

The forward and reverse FCD can be combined by a weighted sum and regarded as a reformulated objective function for ML estimation,

$$R_{FCD}^{ML}(\mathbf{x}(t)) = \frac{w_F}{2\sigma_F^2} D_{FCD}^F(\mathbf{M}(\mathbf{x}(t)), \mathbf{Z}) + \frac{w_R}{2\sigma_R^2} D_{FCD}^R(\mathbf{Z}, \mathbf{M}(\mathbf{x}(t))) \quad (14)$$

where w_F and w_R are weights for the forward and reverse FCD respectively, σ_F and σ_R are constants. The equiva-

lent original objective function based on the reformulation theorem is

$$J_{FCD}^{ML}(\mathbf{F}, \mathbf{Q}, \mathbf{x}(t)) = \frac{w_F}{2\sigma_F^2} \sum_{j=1}^M \beta_j \left[\omega_c^{1-r} f_{j,c}^r \delta + \sum_{i=1}^N \omega_i^{1-r} f_{j,i}^r d(T(\mathbf{m}_j, \mathbf{x}(t)), \mathbf{z}_i) \right] + \frac{w_R}{2\sigma_R^2} \sum_{i=1}^N \alpha_i \left[\pi_c^{1-r} q_{i,c}^r \delta' + \sum_{j=1}^M \pi_j^{1-r} q_{i,j}^r d(\mathbf{z}_i, T(\mathbf{m}_j, \mathbf{x}(t))) \right] \quad (15)$$

subject to $f_{j,c} + \sum_{i=1}^N f_{j,i} = 1$ and $q_{i,c} + \sum_{j=1}^M q_{i,j} = 1$

Prior can also be incorporated and the reformulated objective function with the prior for MAP estimation is

$$R_{FCD}^{MAP}(\mathbf{x}(t)) = R_{FCD}^{ML}(\mathbf{x}(t)) + \frac{1}{2} \|\mathbf{x}(t) - \tilde{\mathbf{x}}(t)\|_{\tilde{\mathbf{P}}(t)}^2 \quad (16)$$

and the equivalent original objective function is

$$J_{FCD}^{MAP}(\mathbf{F}, \mathbf{Q}, \mathbf{x}(t)) = J_{FCD}^{ML}(\mathbf{F}, \mathbf{Q}, \mathbf{x}(t)) + \frac{1}{2} \|\mathbf{x}(t) - \tilde{\mathbf{x}}(t)\|_{\tilde{\mathbf{P}}(t)}^2 \quad (17)$$

where $\tilde{\mathbf{x}}(t) = \mathbf{A}_1 \tilde{\mathbf{x}}(t-1) + \mathbf{A}_2 \tilde{\mathbf{x}}(t-2)$, $\tilde{\mathbf{P}}(t) \approx \mathbf{B}_0 \mathbf{B}_0^T$ are the predicted state vector and covariance respectively.

The reformulated objective functions (14) and (16) can be iteratively minimized via original objective functions (15) and (17) as follows,

Update \mathbf{F} and \mathbf{Q} Given fixed $\mathbf{x}^{(k-1)}(t)$, minimize $J_{FCD}^{ML}(\mathbf{F}, \mathbf{Q}, \mathbf{x}(t))$ or $J_{FCD}^{MAP}(\mathbf{F}, \mathbf{Q}, \mathbf{x}(t))$. Let $T_{\mathbf{u}}(\mathbf{u}_j, \mathbf{x}(t)) = \mathbf{W}_j \mathbf{x}(t)$ is Jacobian of the transformation, at iteration k , $\mathbf{F}^{(k)}$ and $\mathbf{Q}^{(k)}$ can be computed by

$$\begin{aligned} f_{j,i}^{(k)} &\propto \omega_i d(\mathbf{z}_i, T(\mathbf{m}_j, \mathbf{x}^{(k-1)}))^{-\frac{1}{1-r}} & f_{j,c}^{(k)} &\propto \omega_c \delta^{-\frac{1}{1-r}} \\ f_{j,c}^{(k)} + \sum_{i=1}^N f_{j,i}^{(k)} &= 1 \\ q_{i,j}^{(k)} &\propto \pi_j d(\mathbf{z}_i, T(\mathbf{m}_j, \mathbf{x}^{(k-1)}))^{-\frac{1}{1-r}} & q_{i,c}^{(k)} &\propto \pi_c \delta'^{-\frac{1}{1-r}} \\ q_{i,c}^{(k)} + \sum_{j=1}^M q_{i,j}^{(k)} &= 1 \end{aligned} \quad (18)$$

Update $\mathbf{x}(t)$ Given fixed $\mathbf{F}^{(k)}$ and $\mathbf{Q}^{(k)}$, minimize $J_{FCD}^{ML}(\mathbf{F}, \mathbf{Q}, \mathbf{x}(t))$ or $J_{FCD}^{MAP}(\mathbf{F}, \mathbf{Q}, \mathbf{x}(t))$. At iteration k , $\mathbf{x}^{(k)}(t)$ is given by

$$\begin{aligned} \mathbf{x}_{ML}^{(k)}(t) &= \left[\sum_{j=1}^M \mathbf{W}_j^T \tilde{\Sigma}_{\mathbf{u},j}^{(k)-1} \mathbf{W}_j \right]^{-1} \left[\sum_{j=1}^M \mathbf{W}_j^T \tilde{\Sigma}_{\mathbf{u},j}^{(k)-1} \tilde{\mathbf{u}}_j^{(k)} \right] \\ \mathbf{x}_{MAP}^{(k)}(t) &= \left[\tilde{\mathbf{P}}^{-1}(t) + \sum_{j=1}^M \mathbf{W}_j^T \tilde{\Sigma}_{\mathbf{u},j}^{(k)-1} \mathbf{W}_j \right]^{-1} \\ &\times \left[\tilde{\mathbf{P}}^{-1}(t) \tilde{\mathbf{x}}(t) + \sum_{j=1}^M \mathbf{W}_j^T \tilde{\Sigma}_{\mathbf{u},j}^{(k)-1} \tilde{\mathbf{u}}_j^{(k)} \right] \end{aligned} \quad (19)$$

where $\tilde{\mathbf{u}}_j^{(k)} = \frac{\frac{w_F \beta_j}{\sigma_F^2} \sum_{i=1}^N (f_{j,i}^{(k)})^r \omega_i^{1-r} \mathbf{u}_j + \frac{w_R \pi_j}{\sigma_R^2} \sum_{i=1}^N \alpha_i (q_{i,j}^{(k)})^r \mathbf{u}_j}{\frac{w_F \beta_j}{\sigma_F^2} \sum_{i=1}^N (f_{j,i}^{(k)})^r \omega_i^{1-r} + \frac{w_R \pi_j}{\sigma_R^2} \sum_{i=1}^N \alpha_i (q_{i,j}^{(k)})^r}$

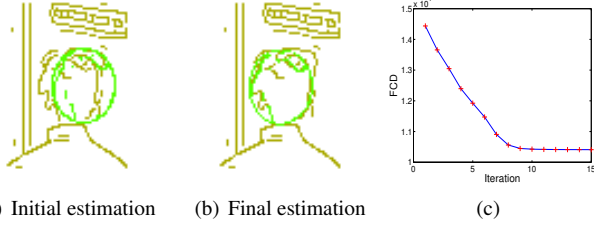


Figure 1. Iterative update where edge measurements are marked in yellow. (a) Initial estimation. (b) Final estimation. (c) FCD decreases monotonically.

$$\text{and } \tilde{\Sigma}_{\mathbf{u},j}^{(k)} = \frac{\Sigma_{\mathbf{u}}}{\frac{w_F \beta_j}{\sigma_F^2} \sum_{i=1}^N (f_{j,i}^{(k)})^r \omega_i^{1-r} + \frac{w_R \pi_j}{\sigma_R^2} \sum_{i=1}^N \alpha_i (q_{i,j}^{(k)})^r}.$$

Note that distances of orientation features only need to be pre-computed once, which then can be used in the iterations to improve the speed. The iterative update is shown in Fig. 1, where $r = 2$, $w_F = 1$, $w_R = 1$ and the reformulated objective function of the combined forward and reverse FCD decreases monotonically.

3.3. Tracking with a probabilistic formulation of the fuzzy chamfer distance

This section presents a probabilistic formulation of the FCD. Based on similarities between the function $F(x)$ of the GM and the kernel function of SVM, a nature extension is to replace the polynomial function in the FCD with a Gaussian. Actually the probabilistic formulation of the forward FCD (forward PFCD) is based on the likelihood of PDA with amplitude information (PDA-AI) [1] to track M independent model samples, where the orientation feature can be regarded as amplitude information. The PDA-AI likelihood for the j th model sample is [1]

$$\begin{aligned} p_j(\mathbf{Z}, N | \mathbf{x}(t)) &= \frac{\mu_F(N)(1-P_D P_G)}{V^N} \prod_{i=1}^N p_0(\mathbf{v}_i) + \frac{\mu_F(N-1)P_D}{N V^{N-1}} \\ &\times \sum_{i=1}^N \mathcal{N}(\mathbf{u}_i; T_{\mathbf{u}}(\mathbf{u}_j, \mathbf{x}(t)), \Sigma_{\mathbf{u}}) K_{\mathbf{v},j}(\mathbf{v}_i; \mathbf{v}_j, \Sigma_{\mathbf{v}}) \prod_{k:k \neq i} p_0(\mathbf{v}_k) \\ &\propto \omega_c p_c + \sum_{i=1}^N \omega_i K_j(\mathbf{z}_i; T(\mathbf{m}_j, \mathbf{x}(t)), \Sigma) \end{aligned} \quad (20)$$

where P_D is the detection probability, P_G is the gating probability, V is the gating volume, $\mu_F(\cdot)$ is the probability mass function of the number of false detections [2], $p_0(\mathbf{v})$ is the probability that \mathbf{v} is from clutter and a uniform distribution $p_0(\mathbf{v}) = p_0$ is used, $\omega_c = 1 - P_D P_G$ and $\omega_i = \frac{1-\omega_c}{N P_G}$, $p_c = \frac{\lambda p_0}{N}$ for Poisson false detection model or $p_c = \frac{p_0}{V}$ for non-parametric false detection model, $K_j(\mathbf{z}_i; T(\mathbf{m}_j, \mathbf{x}(t)), \Sigma) = \mathcal{N}(\mathbf{u}_i; T_{\mathbf{u}}(\mathbf{u}_j, \mathbf{x}(t)), \Sigma_{\mathbf{u}}) K_{\mathbf{v},j}(\mathbf{v}_i; \mathbf{v}_j, \Sigma_{\mathbf{v}})$ and $K_{\mathbf{v},j}(\cdot)$ for the contour model or the edge model was given in [18]. Note that it is indeed in the form of the GM where $F(x) = K_j(x)$ and $h_i = \omega_i$.

So the joint likelihood for all M model samples is

$$\begin{aligned} \mathcal{L}_F(\mathbf{x}(t)) &= \prod_{j=1}^M p_j(\mathbf{Z}, N | \mathbf{x}(t)) \\ &= \prod_{j=1}^M \left[\omega_c p_c + \sum_{i=1}^N \omega_i K_j(\mathbf{z}_i; T(\mathbf{m}_j, \mathbf{x}(t)), \Sigma) \right] \end{aligned} \quad (21)$$

Note that it is similar to the probabilistic formulation of the HD [20, 21] in which the likelihood is

$$\mathcal{L}(\mathbf{x}(t)) = \prod_{j=1}^M [\omega_c p_c + (1 - \omega_c) \mathcal{N}(\mathbf{z}_j^*; T(\mathbf{m}_j, \mathbf{x}(t)), \Sigma)] \quad (22)$$

where $\mathbf{z}_j^* = \min_i d(T(\mathbf{m}_j, \mathbf{x}(t)), \mathbf{z}_i)$ is a nearest neighbor measurement of the transformed model sample $T(\mathbf{m}_j, \mathbf{x}(t))$. However all measurements are involved in the likelihood (21) similar to the FCD (12).

It is also similar to the likelihood used for contour tracking with the CONDENSATION algorithm [17] where measurements $\mathbf{Z}(\mathbf{x}(t))$ are restricted to be on normal lines of contour samples and are a function of the state vector $\mathbf{x}(t)$ which is a drawback from the perspective of Bayesian inference. Now measurements are fixed in the likelihood (21) and are not restricted to be on normal lines of contour samples due to the employment of the orientation feature and model samples now include not only contour samples but also edge pixels inside.

In practice the independent assumption is not valid if model samples are close to each other and model samples may be weighted to emphasis matching of model samples with higher weights, the likelihood becomes

$$\begin{aligned} \mathcal{L}_F(\mathbf{x}(t)) &= \prod_{j=1}^M p_j(\mathbf{Z}, N | \mathbf{x}(t))^{\beta_j} \\ &= \prod_{j=1}^M \left[\omega_c p_c + \sum_{i=1}^N \omega_i K_j(\mathbf{z}_i; T(\mathbf{m}_j, \mathbf{x}(t)), \Sigma) \right]^{\beta_j} \end{aligned} \quad (23)$$

where β_j is the weight for the j th model sample.

The likelihood based on Probabilistic Multi-Hypothesis Tracker (PMHT) in [18] can be regarded as a reverse PFCD,

$$\mathcal{L}_R(\mathbf{x}(t)) = \prod_{i=1}^N \left[\pi_c p'_c + \sum_{j=1}^M \pi_j K_j(\mathbf{z}_i; T(\mathbf{m}_j, \mathbf{x}(t)), \Sigma) \right]^{\alpha_i} \quad (24)$$

A reformulated objective function combining the likelihood of the forward PFCD (23) and the likelihood of the reverse PFCD (24) is

$$R_{PFCD}^{ML}(\mathbf{x}(t)) = -\frac{w_F}{2\sigma_F^2} \log \mathcal{L}_F(\mathbf{x}(t)) - \frac{w_R}{2\sigma_R^2} \log \mathcal{L}_R(\mathbf{x}(t)) \quad (25)$$

and the equivalent original objective function for ML esti-

mation is

$$\begin{aligned}
& J_{PFCD}^{ML}(\mathbf{x}(t)) = \\
& - \sum_{j=1}^M \beta_j \left[\sum_{i=1}^N f_{j,i} \log \frac{\omega_i K_j(\mathbf{z}_i; T(\mathbf{m}_j, \mathbf{x}(t)), \Sigma)}{f_{j,i}} + f_{j,c} \log \frac{\omega_c p_c}{f_{j,c}} \right] \\
& - \sum_{i=1}^N \alpha_j \left[\sum_{j=1}^M q_{i,j} \log \frac{\pi_j K_j(\mathbf{z}_i; T(\mathbf{m}_j, \mathbf{x}(t)), \Sigma)}{q_{i,j}} + q_{i,c} \log \frac{\pi_c p'_c}{q_{i,c}} \right] \\
& \text{subject to } f_{j,c} + \sum_{i=1}^N f_{j,i} = 1 \text{ and } q_{i,c} + \sum_{j=1}^M q_{i,j} = 1
\end{aligned} \tag{26}$$

Rather than the ML estimation in [20], the prior is important for tracking and can be incorporated into the posterior, which is equivalent to a reformulated objective function

$$R_{PFCD}^{MAP}(\mathbf{x}(t)) = R_{PFCD}^{ML}(\mathbf{x}(t)) + \frac{1}{2} \|\mathbf{x}(t) - \tilde{\mathbf{x}}(t)\|_{\tilde{\mathbf{P}}(t)}^2 \tag{27}$$

and the equivalent original objective function for MAP estimation is

$$J_{PFCD}^{MAP}(\mathbf{F}, \mathbf{x}(t)) = J_{PFCD}^{ML}(\mathbf{x}(t)) + \frac{1}{2} \|\mathbf{x}(t) - \tilde{\mathbf{x}}(t)\|_{\tilde{\mathbf{P}}(t)}^2 \tag{28}$$

The reformulated objective functions (25) and (27) can be iteratively minimized via original objective functions (26) and (28) as follows,

Update \mathbf{F} and \mathbf{Q} Given fixed $\mathbf{x}^{(k-1)}(t)$, minimize $J_{PFCD}^{ML}(\mathbf{F}, \mathbf{Q}, \mathbf{x}(t))$ or $J_{PFCD}^{MAP}(\mathbf{F}, \mathbf{Q}, \mathbf{x}(t))$. At iteration k , $\mathbf{F}^{(k)}$ and $\mathbf{Q}^{(k)}$ can be computed by

$$\begin{aligned}
& f_{j,i}^{(k)} \propto \omega_i K_j(\mathbf{z}_i; T(\mathbf{m}_j, \mathbf{x}^{(k-1)}(t)), \Sigma) \quad f_{j,c}^{(k)} \propto \omega_c p_c \\
& f_{j,c}^{(k)} + \sum_{i=1}^M f_{j,i}^{(k)} = 1 \\
& q_{i,j}^{(k)} \propto \pi_j K_j(\mathbf{z}_i; T(\mathbf{m}_j, \mathbf{x}^{(k-1)}(t)), \Sigma) \quad q_{i,c}^{(k)} \propto \pi_c p'_c \\
& q_{i,c}^{(k)} + \sum_{i=1}^N q_{i,j}^{(k)} = 1
\end{aligned} \tag{29}$$

Update $\mathbf{x}(t)$ Given fixed $\mathbf{F}^{(k)}$ and $\mathbf{Q}^{(k)}$, minimize $J_{PFCD}^{ML}(\mathbf{F}, \mathbf{Q}, \mathbf{x}(t))$ or $J_{PFCD}^{MAP}(\mathbf{F}, \mathbf{Q}, \mathbf{x}(t))$. At iteration k , $\mathbf{x}^{(k)}(t)$ is given by

$$\begin{aligned}
& \mathbf{x}_{ML}^{(k)}(t) = \left[\sum_{j=1}^M \mathbf{W}_j^T \tilde{\Sigma}_{\mathbf{u},j}^{(k)-1} \mathbf{W}_j \right]^{-1} \left[\sum_{j=1}^M \mathbf{W}_j^T \tilde{\Sigma}_{\mathbf{u},j}^{(k)-1} \tilde{\mathbf{u}}_j^{(k)} \right] \\
& \mathbf{x}_{MAP}^{(k)}(t) = \left[\tilde{\mathbf{P}}^{-1}(t) + \sum_{j=1}^M \mathbf{W}_j^T \tilde{\Sigma}_{\mathbf{u},j}^{(k)-1} \mathbf{W}_j \right]^{-1} \\
& \times \left[\tilde{\mathbf{P}}^{-1}(t) \tilde{\mathbf{x}}(t) + \sum_{j=1}^M \mathbf{W}_j^T \tilde{\Sigma}_{\mathbf{u},j}^{(k)-1} \tilde{\mathbf{u}}_j^{(k)} \right]
\end{aligned} \tag{30}$$

where $\tilde{\mathbf{u}}_j^{(k)} = \frac{\frac{w_F \beta_j}{2\sigma_F^2} \sum_{i=1}^N f_{j,i}^{(k)} \mathbf{u}_j + \frac{w_R}{2\sigma_R^2} \sum_{i=1}^N \alpha_i q_{i,j}^{(k)} \mathbf{u}_j}{\frac{w_F \beta_j}{2\sigma_F^2} \sum_{i=1}^N f_{j,i}^{(k)} + \frac{w_R}{2\sigma_R^2} \sum_{i=1}^N \alpha_i q_{i,j}^{(k)}}$ and $\tilde{\Sigma}_{\mathbf{u},j}^{(k)} = \frac{\Sigma_{\mathbf{u}}}{\frac{w_F \beta_j}{2\sigma_F^2} \sum_{i=1}^N f_{j,i}^{(k)} + \frac{w_R}{2\sigma_R^2} \sum_{i=1}^N \alpha_i q_{i,j}^{(k)}}$.

The main stages of tracking with the FCD/PFCD are summarized in algorithm 1.

Algorithm 1 Tracking with the Fuzzy Chamfer Distance and its Probabilistic Formulation

1. Prediction
 2. Iterative optimization
 - $k = 1, \mathbf{x}^{(0)}(t) = \tilde{\mathbf{x}}(t)$
 - (i) Update \mathbf{F} and \mathbf{Q} by equation (18) or equation (29)
 - (ii) Update $\mathbf{x}(t)$ by equation (19) or equation (30)
 - if** $\|\mathbf{x}^{(k)}(t) - \mathbf{x}^{(k-1)}(t)\| < \varepsilon$, **then**
 - $\hat{\mathbf{x}}(t) = \mathbf{x}^{(k)}(t)$ and stop
 - else**
 - $k = k + 1$ go to (i)
 - end if**
-

4. Results and discussions

Fuzzy chamfer distance/Chamfer distance and Hausdorff distance The DT is essential for tracking with the CD [24], the HD [15] or its probabilistic formulation [20, 21], so that a multi-resolution search algorithm or particle filters can be used efficiently based on the DT. However for the DT, only low dimensional feature vectors can be employed as the complexity of the DT grows rapidly with the dimensionality of feature vectors. In addition, the complexity of multi-resolution search or particle filters also grows rapidly with the dimensionality of state vectors, due to the curse of dimensionality.

On the contrary, the DT is not useful for the FCD/PFCD, as distances from all model samples to all measurements have to be computed. Higher dimensional feature vectors can be employed, as distances of feature vectors only need to be computed once and are then used in iterative algorithms, which usually only take a few iterations and now it can track two or three objects in near real time on 3GHz Pentium IV. Due to a monotonicity property of the iterative algorithm, it can seek the mode of likelihoods or posteriors despite high dimensional state space and sharply peaked likelihoods, which may be difficult for tracking with multi-resolution search and particle filters.

As only forward distance is usually used in previous work on tracking with the CD [24] or the HD [15, 20], for a fair comparison, results of tracking with the forward PFCD only ($w_F = 1$ and $w_R = 0$) using iterative algorithm 1 on CAVIAR¹ “TwoEnterShop1cor” and “seq_sb”² are shown in Fig. 2 (a) and Fig. 3 (a). A head in green ellipse and a head in red ellipse make dramatic appearance changes in CAVIAR “TwoEnterShop1cor” while a head is occluded by unknown objects four times in “seq_sb”. Examples of

¹The EC Funded CAVIAR project/IST 2001 37540, see <http://homepages.inf.ed.ac.uk/rbf/CAVIAR/>.

²The sequence is from <http://vision.stanford.edu/birch/headtracker/>.

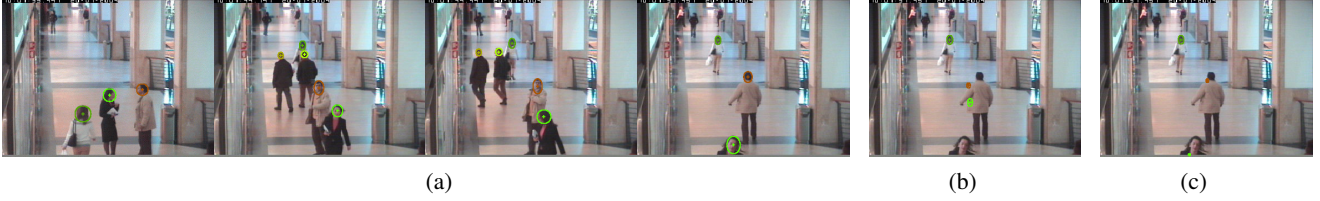


Figure 2. Results of CAVIAR “TwoEnterShop1cor”. (a) Tracking with the forward PFCD. (b)(c) Examples of tracking failure with the multi-channel chamfer distance and the probabilistic formulation of the Hausdorff distance using the SIR particle filter respectively.

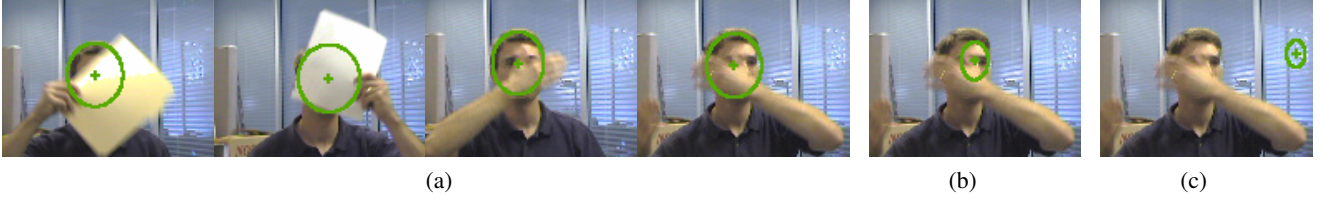


Figure 3. Results of “seq_sb”. (a) Tracking with the forward PFCD. (b)(c) Examples of tracking failure with the multi-channel chamfer distance and the probabilistic formulation of the Hausdorff distance using the SIR particle filter respectively.



Figure 4. Comparison of (a) Tracking with the forward PFCD. (b) Tracking with the reverse PFCD.

tracking failure under dramatic appearance changes and heavy occlusions, for the multi-channel chamfer distance [24] and the likelihood (22) of the probabilistic formulation of the HD [20] using SIR particle filters, are given in Fig. 2 (b)(c) and Fig. 3 (b)(c) respectively.

Forward/Reverse One issue of the forward FCD/PFCD (actually also for the forward CD [24], the partial forward HD [15] and its probabilistic formulation [20, 21]) is that there is no exclusion principle as that of Joint Probabilistic Data Association (JPDA) [2] and PMHT [25], so one measurement may be associated with multiple model samples. On the contrary, the reverse FCD/PFCD has the exclusion principle so that one measurement can only be associated with one model sample, which make it more suitable for tracking multiple objects jointly during occlusions as shown in Fig. 4, where an object in red is tracked through occlusions with the likelihood (24) of reverse PFCD rather than with the likelihood (23) of forward PFCD. For this reason, only the reverse FCD/PFCD is used when a cluster contains more than one object so multiple objects are jointly tracked with the reverse FCD/PFCD as that of [18]. The forward FCD/PFCD can be used alone or with the reverse FCD/PFCD to track multiple single objects when there is only one object in a cluster.

Three results of multi-object tracking on challenging sequences with both the forward and reverse PFCD are shown in Fig. 5, Fig. 6 and Fig. 7, where multiple single objects are tracked with the forward PFCD only while multiple ob-

jects in the same cluster, linked by white lines, are jointly tracked with the reverse PFCD only. Fig. 5 shows results on “office”, in which there are dramatic appearance changes, scale changes and four heavy occlusions from frame 5280 to 5320, from frame 5340 to 5370, from frame 5380 to 5410 and from frame 5410 to 5424.

Fig. 6 shows results on CAVIAR “OneShopOneWait2-cor” where head sizes are quite small and there are two heavy occlusions from frame 1166 to 1176 and from frame 1276 to 1292.

Fig. 7 shows results of tracking with the B-spline model on CAVIAR “OneStopMoveEnter1cor”, which is a very challenging sequence with a very crowded and cluttered scene, and there are four heavy occlusions, from frame 916 to 954, from frame 956 to 974, from frame 1152 to 1176 and from frame 1184 to 1218. These results show the effectiveness of both forward and reverse PFCD.

5. Conclusions

This paper introduces the FCD/PFCD for edge-based visual tracking. First, connections of the CD/HD with fuzzy objective functions for clustering are shown with the reformulation theorem. The FCD based on fuzzy objective functions and the PFCD based on data association methods are then presented for tracking, which can all be regarded as reformulated fuzzy objective functions and minimized with iterative algorithms. Results on challenging sequences show the performance of the proposed tracking method.

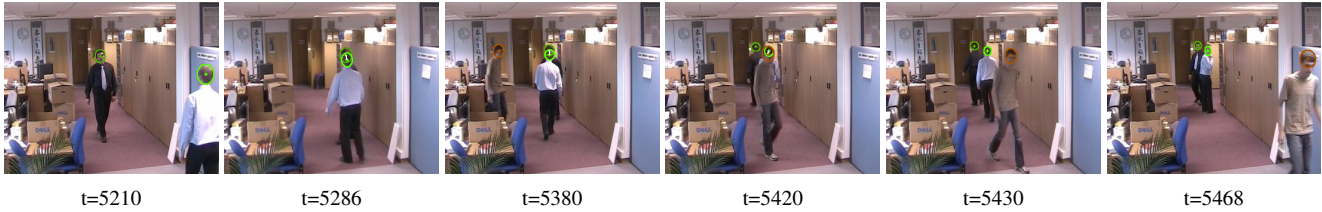


Figure 5. Results of “office” with the forward and reverse PFCD. ©Mitsubishi Electric ITE 2005.



Figure 6. Results of CAVIAR “OneShopOneWait2cor” with the forward and reverse PFCD.



Figure 7. Results of CAVIAR “OneStopMoveEnter1cor” with the forward and reverse PFCD.

References

- [1] Y. Bar-Shalom. *Multitarget-Multisensor Tracking: Principles and Techniques*. YBS, 1995.
- [2] Y. Bar-Shalom and T. Fortmann. *Tracking and Data Association*. Academic Press, 1988.
- [3] A. M. Baumberg and D. C. Hogg. Learning flexible models from image sequences. In *Proc. ECCV*, pages 299–308, 1994.
- [4] J. C. Bezdek. *Pattern Recognition with Fuzzy Objective Function Algorithms*. Plenum Press, 1981.
- [5] A. Blake, R. Curwen, and A. Zisserman. A framework for spatio-temporal control in the tracking of visual contours. *IJCV*, 11(2):127–145, 1993.
- [6] A. Blake and M. Isard. *Active Contours*. Springer, 1998.
- [7] G. Borgefors. Hierarchical chamfer matching: a parametric edge matching algorithm. *IEEE PAMI*, 10(6):849–865, Nov. 1988.
- [8] J. Canny. A computational approach to edge detection. *IEEE PAMI*, 8(6):679–698, Nov. 1986.
- [9] R. N. Davé. Characterization and detection of noise in clustering. *Pattern Recognition Letters*, 12(11):657–664, 1991.
- [10] M.-P. Dubuisson and A. K. Jain. A modified Hausdorff distance for object matching. In *Proc. ICPR*, pages 566–568, 1994.
- [11] D. M. Gavrilu and V. Philomin. Real-time object detection for “smart” vehicles. In *Proc. IEEE ICCV*, pages 87–93, 1999.
- [12] D. E. Goldberg. *Genetic Algorithms in Search, Optimization and Machine Learning*. Addison Wesley, 1989.
- [13] R. J. Hathaway and J. C. Bezdek. Optimization of clustering criteria by reformulation. *IEEE Transactions on Fuzzy Systems*, 3(2):241–246, 1995.
- [14] D. P. Huttenlocher, G. A. Klanderman, and W. J. Rucklidge. Comparing images using the Hausdorff distance. *IEEE PAMI*, 15(9):850–863, September 1993.
- [15] D. P. Huttenlocher, J. J. Noh, and W. J. Rucklidge. Tracking non-rigid objects in complex scenes. In *Proc. IEEE ICCV*, pages 93–101, 1993.
- [16] D. P. Huttenlocher and W. J. Rucklidge. A multi-resolution technique for comparing images using the Hausdorff distance. In *Proc. IEEE CVPR*, pages 705–706, 1993.
- [17] M. Isard and A. Blake. Contour tracking by stochastic propagation of conditional density. In *Proc. ECCV*, pages 343–356, 1996.
- [18] Y. Jin and F. Mokhtarian. Variational particle filter for multi-object tracking. In *Proc. IEEE ICCV*, 2007.
- [19] O. Nasraoui and R. Krishnapuram. A genetic algorithm for robust clustering based on a fuzzy least median of squares criterion. In *Proc. NAFIPS Conference*, pages 217–221, 1997.
- [20] C. F. Olson. A probabilistic formulation for Hausdorff matching. In *Proc. IEEE CVPR*, pages 150–156, 1998.
- [21] C. F. Olson. Maximum-likelihood image matching. *IEEE PAMI*, 24(6):853–857, June 2002.
- [22] A. E. C. Pece and A. D. Worrall. Tracking with the EM contour algorithm. In *Proc. ECCV*, pages 3–17, 2002.
- [23] W. J. Rucklidge. Locating objects using the Hausdorff distance. In *Proc. IEEE ICCV*, pages 457–464, 1995.
- [24] B. Stenger, A. Thayananthan, P. H. S. Torr, and R. Cipolla. Filtering using a tree-based estimator. In *Proc. IEEE ICCV*, pages 1063–1070, 2003.
- [25] R. Streit and T. Luginbuhl. Maximum likelihood method for probabilistic multi-hypothesis tracking. *Proc. SPIE*, 2235:394–405, 1994.